

# Adiponectin inhibits LPS-induced nucleus pulposus cell pyroptosis through the miR-135a-5p/TXNIP signaling pathway

Shuang Wu<sup>1</sup>, Shida Liu<sup>1</sup>, Rui Huang<sup>1</sup>, Youbing Zhou<sup>1</sup>, Yongcheng Zou<sup>1</sup>, Wei Yang<sup>1</sup>, Jian Zhang<sup>1</sup>

<sup>1</sup>The First Affiliated Hospital, Orthopedic Center, Hengyang Medical School, University of South China, Hengyang 421001, Hunan, China

**Correspondence to:** Jian Zhang; email: [462192195@qq.com](mailto:462192195@qq.com), <https://orcid.org/0009-0002-7423-2018>

**Keywords:** IDD, APN, miR-135a-5p, TXNIP, pyroptosis

**Received:** August 7, 2023

**Accepted:** October 15, 2023

**Published:** December 2, 2023

**Copyright:** © 2023 Wu et al. This is an open access article distributed under the terms of the [Creative Commons Attribution License](https://creativecommons.org/licenses/by/4.0/) (CC BY 4.0), which permits unrestricted use, distribution, and reproduction in any medium, provided the original author and source are credited.

## ABSTRACT

Pyroptosis, a newly discovered programmed cell death process, is characterized by NLRP3 inflammasome activation and pro-inflammatory mediator release. Nucleus pulposus (NP) cell pyroptosis is an important cause of intervertebral disc degeneration (IDD). Adiponectin (APN) is an adipokine and has an anti-inflammatory effect. However, whether and how APN protects against NP cell pyroptosis remains unexplored. Our results showed that human degenerated NP tissue displayed a significant increase in the protein levels of NLRP3, caspase-1 and GSDMD-N. APN expression was down-regulated in human degenerated NP tissue and NP cells challenged with lipopolysaccharide (LPS). Lentivirus-mediated overexpression of APN increased miR-135a-5p levels, decreased thioredoxin-interacting protein (TXNIP) expression and its interaction with NLRP3, and inhibited pyroptosis in human NP cells stimulated with LPS. TXNIP was identified as a direct target of miR-135a-5p. The inhibitory effects of APN on pyroptosis were reversed by pretreatment with miR-135a-5p inhibitor or lentiviral vector expressing TXNIP in LPS-treated human NP cells. In summary, these data suggest that APN restrains LPS-induced pyroptosis through the miR-135a-5p/TXNIP signaling pathway in human NP cells. Increasing APN levels could be a new approach to retard IDD.

## INTRODUCTION

As a global challenge, low back pain (LBP) has a considerable effect on economy and society. LBP is predominantly caused by intervertebral disc degeneration (IDD). Cell death and inflammatory response are regarded as two critical pathological mechanisms for IDD [1, 2]. Increased cell death is frequently observed in human degenerated intervertebral disc (IVD) samples and animal models [3, 4]. Pyroptosis is an inflammatory cell death manner. In this process, interleukin (IL)-1 $\beta$  and IL-18 are abundantly released. Nucleus pulposus (NP), the major structural component, is a gelatinous matrix. NP cell pyroptosis has been thought to be a critical contributor to IDD [5, 6].

Adiponectin (APN) is an adipokine with an anti-inflammatory effect [7]. APN is down-regulated in

human degenerated IVD, and its levels are negatively correlated with degeneration degree [8]. A strong association exists between circulating APN levels and lumbar disc degeneration [9]. Treatment with APN inhibits NLRP3 inflammasome activation and prevents human aortic epithelial cells from lipopolysaccharide (LPS)-induced pyroptosis [10]. APN also suppresses LPS-induced pyroptosis of vascular smooth muscle cells [11]. However, whether APN can modulate NP cell pyroptosis is unclear.

Dysregulation of miRNAs is known to be involved in IDD progression [12–14]. miR-135a-5p is a pleiotropic miRNA. Activation of farnesoid X receptor alleviates vascular inflammation by increasing miR-135a-5p levels in rats with chronic kidney disease [15]. Thioredoxin-interacting protein (TXNIP) can combine with NLRP3 to induce pyroptosis [16, 17]. Administration of morin

diminishes NP cell pyroptosis and mitigates IDD in mice by inhibiting the TXNIP/NLRP3 signaling pathway [18]. Conversely, propionibacterium acnes induces NP cell pyroptosis and promotes the degeneration of IVD in a rabbit model of IDD by activating this pathway [19]. However, whether the miR-135a-5p/TXNIP signaling cascade is associated with APN-regulated NP cell pyroptosis is still elusive. The objective of this research was to explore whether APN can affect NP cell pyroptosis.

## MATERIALS AND METHODS

### Cells, reagents and antibodies

We obtained 293T cells from American Type Culture Collection (Rockville, MD, USA). Lentiviral vector expressing APN or TXNIP was synthesized by Genechem (Shanghai, China). Dulbecco's Modified Eagle Medium (DMEM)/F12 (Gibco, Grand Island, NY, US), Hoechst 33342/propidium iodide (PI) double stain kit (Solarbio, Beijing, China), Lipofectamine 3000 (Invitrogen, Carlsbad, CA, USA), miR-135a-5p mimic/inhibitor (Ribobio, Guangzhou, China), dual-luciferase reporter assay system (Promega, Madison, WI, USA), lactate dehydrogenase (LDH) assay kit (Beyotime, Shanghai, China), enzyme-linked immunosorbent assay (ELISA) kits (R&D systems, Minneapolis, MN, USA), polyvinylidene difluoride (PVDF) membranes (Millipore, Billerica, MA, USA), and horseradish peroxidase-conjugated goat anti-rabbit IgG (Proteintech, Chicago, IL, USA) were obtained as indicated. Fetal bovine serum (FBS), trypsin, type II collagenase and LPS were purchased from Sigma-Aldrich (St. Louis, MO, USA). Rabbit antibodies against APN, TXNIP, NLRP3, caspase-1, Gasdermin N-terminal fragment (GSDMD-N), and  $\beta$ -actin were supplied by Abcam (Cambridge, UK).

### NP tissue sample collection

The patients with lumbar vertebral fracture (LVF) or IDD were collected from the First Affiliated Hospital of University of South China. Information regarding these patients is listed in Supplementary Table 1. NP tissue was carefully isolated after surgery.

### Cell culture and transfection

After washing with phosphate buffered saline (PBS), normal NP tissue were cut into pieces, digested, and then centrifuged at 600 g to collect cells. The isolated NP cells were cultured and passaged. We selected the second-generation cells to perform the *in vitro* experiments. Cells were treated with 1  $\mu$ g/mL of

LPS to induce pyroptosis. Twelve h later, cells were transfected with 100 MOI of lentiviral vector expressing APN or empty vector. After 24 h, the transfection effect was evaluated by detecting APN protein levels.

For overexpression of TXNIP, human NP cells were transduced with 100 MOI of TXNIP-expressing lentivirus or empty vector. To overexpress or silence miR-135a-5p, human NP cells were transfected with miR-135a-5p mimic or its inhibitor (40 nM) at the aid of Lipofectamine 3000. Following 24 h of treatment, TXNIP protein and miR-135a-5p expression was measured for determination of transfection effect.

### Bioinformatics analysis and luciferase reporter detection

The interaction of miR-135a-5p with TXNIP 3'UTR was analyzed by three online databases: TargetScan, miRDB and RNAhybrid. Next, we assayed the luciferase activity according to a previously reported method [20]. Briefly, TXNIP-WT and TXNIP-Mut plasmids were constructed. By using Lipofectamine 3000, these plasmids were cotransfected into 293T cells with miR-135a-5p mimic. Following 24 h, luciferase activity was measured.

### Hoechst 33342/PI fluorescence staining

At the end of treatment, human NP cells were harvested. Hoechst 33342 solution (5  $\mu$ L) was added to cells. After 20 min of staining, 5  $\mu$ L of PI was added to cells. Fifteen min later, cells were photographed.

### LDH detection

The cell culture supernatants were collected. After centrifugation, supernatants were incubated with LDH test working solution (60  $\mu$ L) for 30 min, followed by measurement of absorbance at 490 nm using spectrophotometric microplate reader [21].

### ELISA

The secretion of IL-1 $\beta$  and IL-18 was assessed by the ELISA kits.

### Co-immunoprecipitation (Co-IP) assay

Cells were lysed and then incubated with anti-TXNIP or anti-NLRP3 antibodies overnight. Dynabeads protein G was added. After washing, immunoprecipitates were eluted at 60° C for 5 min with 40 mL of 1  $\times$  SDS sample buffer, followed by immunoblotting analysis of TXNIP and NLRP3.

## qRT-PCR

For extracting total RNA in tissue and cells, the TRIzol kit was utilized. After conversion to cDNA, qRT-PCR was carried out and target gene expression was quantified using GAPDH or U6 as internal controls. The primer sequences were as follows: APN (F: 5'-T TGGTCTA AGGGAGACATCG-3', R: 5'-CACAC TGAATGCTGAGCGGTA-3'), TXNIP (F: 5'-C AGAA GCTCCTCCCTGCTATATG-3', R: 5'-GATGCAGGG ATCCACCTCAG-3'), GAPDH (F: 5'-TGTGGGCA TCAATGGATTTGG-3', R: 5'-ACACCATGTATTCC GGGTCAA T-3'), miR-135a-5p (F: 5'-CTCCTAGGT ATGGCTTTTTATTTC-3', R: 5'-TCAACTG GTGTCG TGGAGTC-3'), and U6 (F: 5'-AGTAAGCCCTTG CTGTCAGTG-3', R: 5'-CCTGGGTCTGATAATGCT GGG-3').

## Western blot

The RIPA buffer was used to isolate total proteins from tissue and cells, which was accompanied by protein concentration detection. Subsequently, SDS-PAGE was employed to separate proteins, which

were diverted to PVDF membranes. Following blockade, the PVDF membranes were incubated with the primary antibodies and then secondary antibody. Immunoreactive bands were developed using BeyoECL Plus kit (Beyotime).

## Statistical analyses

The experimental data are expressed as the mean  $\pm$  standard deviation from at least 3 separate experiments. Differences among groups were analyzed by Student's *t*-test or one-way ANOVA followed by Tukey's multiple comparison test. The statistical analyses were conducted using GraphPad Prism 8.0 software.  $P < 0.05$  was thought to have statistical significance.

## RESULTS

### APN is down-regulated in degenerated NP tissue and LPS-stimulated NP cells

NP tissue was isolated from LVF and IDD patients. Figure 1A shows increased NLRP3, caspase-1 and GSDMD-N expression in human degenerated NP tissue,

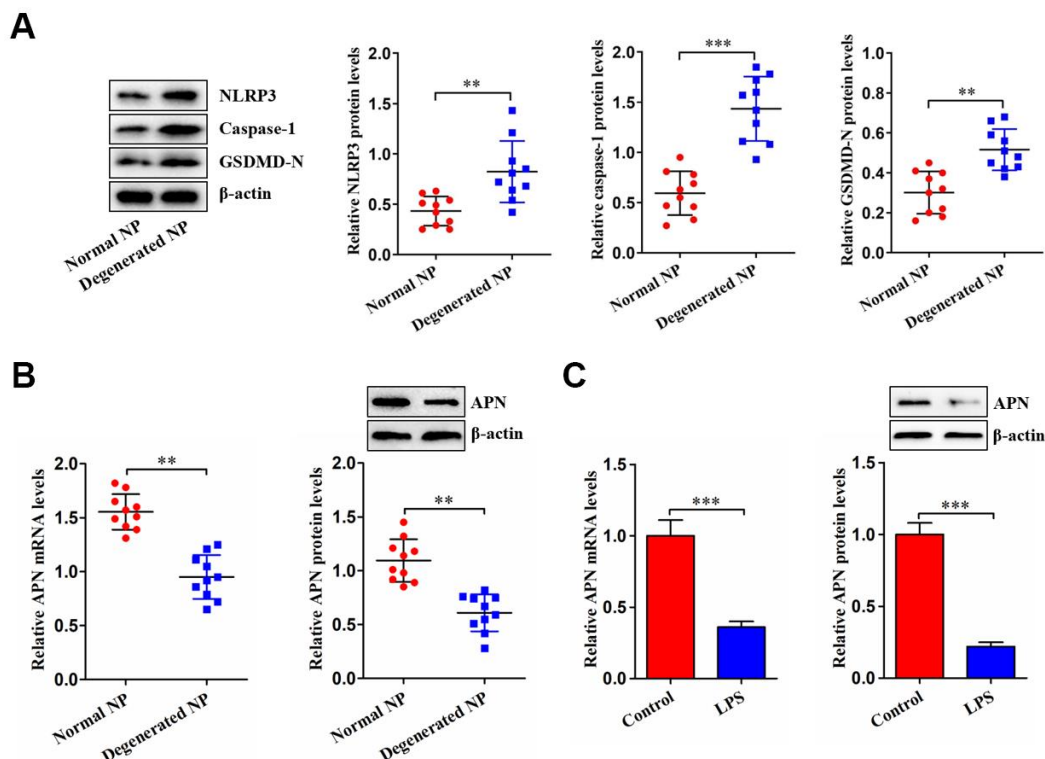


**Figure 1. Decreased APN expression in degenerated NP tissue and LPS-treated human NP cells.** (A) Western blot was used to determine the protein levels of NLRP3, caspase-1 and GSDMD-N in normal and degenerated human NP tissue samples ( $n=10$ ). (B) The qRT-PCR and western blot analyses of APN expression in normal and degenerated human NP tissue samples ( $n=10$ ). (C) Human NP cells were treated with PBS or LPS for 12 h, followed by measurement of APN expression using qRT-PCR and western blot ( $n=3$ ). Data are expressed as mean  $\pm$  SD. \*\* $P < 0.01$ , \*\*\* $P < 0.001$ .

indicating that NP cell pyroptosis is increased during IDD. We next measured APN expression in NP tissue as well as LPS-stimulated NP cells. Decreased APN expression was observed in degenerated NP tissue (Figure 1B). Consistently, stimulation of human NP cells with LPS dramatically attenuated APN levels (Figure 1C). Thus, APN may be involved in IDD progression.

### APN inhibits LPS-induced pyroptosis in human NP cells

APN overexpression led to a marked elevation of APN protein levels, as evidenced by western blot (Figure 2A). LPS stimulation dramatically up-regulated NLRP3, caspase-1 and GSDMD-N expression, while this up-regulation was alleviated by APN overexpression

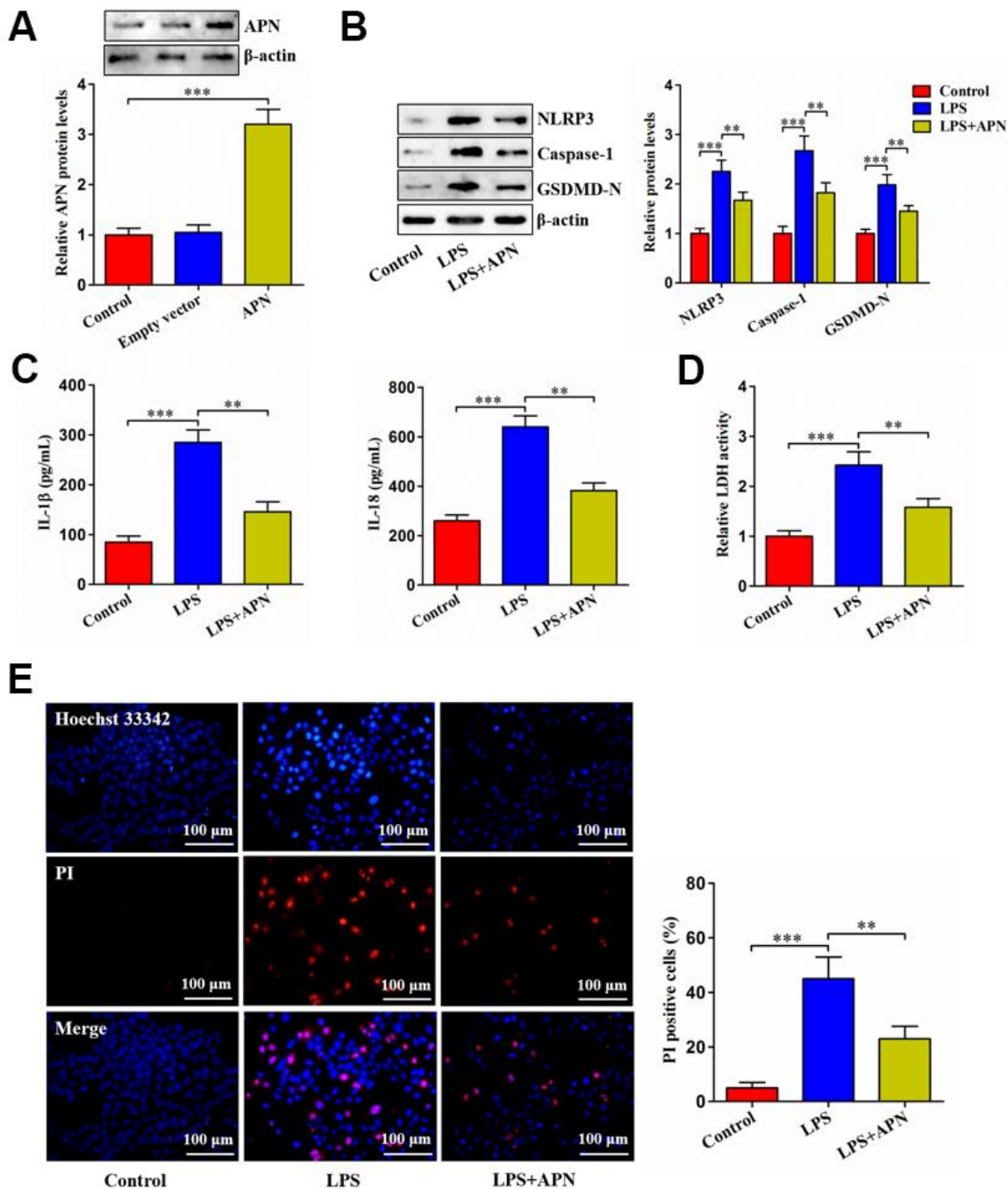


**Figure 2. Effects of APN on LPS-induced human NP cell pyroptosis.** (A) Human NP cells were incubated with PBS, empty vector or lentiviral vector expressing APN for 24 h. Protein samples were immunoblotted with antibodies against APN or  $\beta$ -actin. (B–E) Human NP

cells were treated with PBS or LPS for 12 h, followed by transduction with or without APN-expressing lentivirus for 24 h. (B) The western blot analysis of NLRP3, caspase-1 and GSDMD-N protein expression. (C) ELISA was used to determine IL-1 $\beta$  and IL-18 levels in the cell culture supernatants. (D) Detection of LDH activity in the cell culture supernatants using an LDH assay kit. (E) Representative images of fluorescent staining with Hoechst 33342 (blue) and PI (red) and quantitative analysis of PI positive cells. All data are presented as mean  $\pm$  SD from three independent experiments. \*\* $P$  < 0.01, \*\*\* $P$  < 0.001.

(Figure 2B). Accordingly, APN overexpression reversed LPS-induced enhancement of IL-1 $\beta$  and IL-18 secretion (Figure 2C). Consistently, increased LDH release by LPS was alleviated by APN overexpression (Figure 2D). APN overexpression also reduced pyroptotic cell death caused by LPS (Figure 2E). To summarize, APN contributes to inhibition of LPS-induced human NP cell pyroptosis.

### APN decreases TXNIP expression and inhibits its interaction with NLRP3

Upon binding to NLRP3, TXNIP can induce cell pyroptosis. We inferred that APN inhibits LPS-induced human NP cell pyroptosis possibly through TXNIP. The expression of TXNIP was first detected in NP tissue. As anticipated, TXNIP was highly expressed in degenerated NP tissue samples (Figure 3A). Then, we transfected APN-expressing

lentivirus into LPS-treated human NP cells. LPS stimulation dramatically elevated TXNIP mRNA and protein levels, which was alleviated by APN overexpression (Figure 3B). The Co-IP experiment further revealed that APN overexpression reduced the interaction between TXNIP and NLRP3 (Figure 3C). These data indicate that APN down-regulates TXNIP expression and suppresses the binding of TXNIP to NLRP3 in human NP cells stimulated with LPS.

### TXNIP is involved in APN-induced inhibition of human NP cell pyroptosis

Given the above studies have identified APN as a negative regulator of TXNIP, we overexpressed TXNIP through a lentiviral vector in human NP cells (Figure 4A). LPS-treated human NP cells were then transduced with lentiviral vector expressing TXNIP,

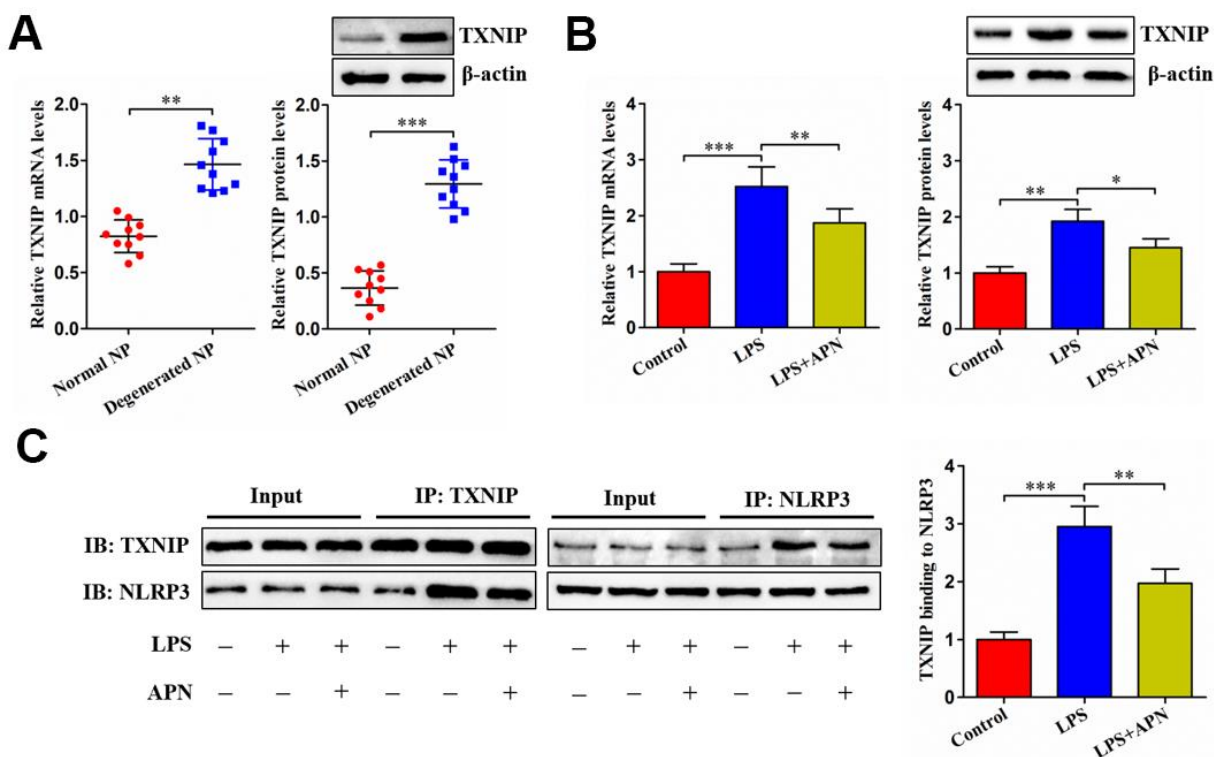


**Figure 3. Effects of APN on TXNIP expression and its interaction with NLRP3.** (A) TXNIP expression was assayed by qRT-PCR and western blot in normal and degenerated human NP tissue samples ( $n=10$ ). (B, C) After 12 h of treatment with PBS or LPS, human NP cells were transfected with or without lentiviral vector expressing APN for 24 h ( $n=3$ ). (B) TXNIP expression was evaluated by qRT-PCR and western blot. (C) Co-IP analysis of TXNIP interaction with NLRP3. All results are expressed as the mean  $\pm$  SD. \* $P$  < 0.05, \*\* $P$  < 0.01, \*\*\* $P$  < 0.001.

followed by treatment with lentiviral vector expressing APN. TXNIP overexpression reduced the influence of APN on pyroptosis-related protein expression (Figure 4B). Additionally, APN overexpression reduced extra-cellular IL-1 $\beta$ , IL-18 and LDH contents as well as

suppressed pyroptotic cell death, both of which were reversed by pretreatment with lentiviral vector expressing TXNIP (Figure 4C–4E). Thus, TXNIP is required for the prevention of human NP cell pyroptosis induced by APN.

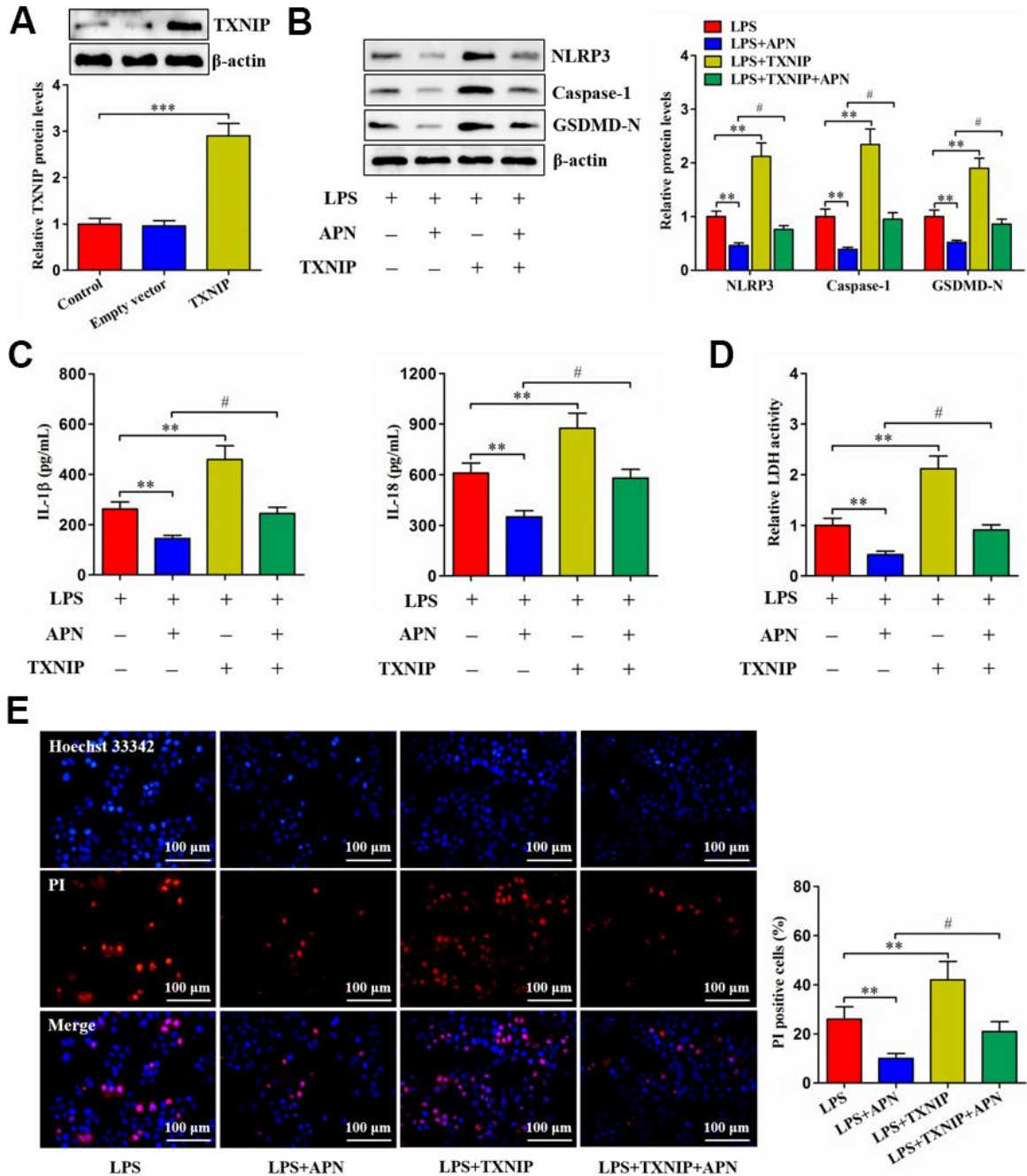


**Figure 4. Involvement of TXNIP in APN-inhibited human NP cell pyroptosis.** (A) Human NP cells were treated with PBS, empty vector or lentiviral vector expressing TXNIP for 24 h, followed by western blot analysis of TXNIP protein. (B–E) Human NP cells were transfected with APN and/or TXNIP by lentiviral vector in the presence of LPS. (B) Cell lysates were immunoblotted with indicated antibodies. (C) The levels of IL-1 $\beta$  and IL-18 were detected using ELISA in the cell culture supernatants. (D) The LDH assay kit was employed to measure LDH activity in the cell culture supernatants. (E) Representative images of fluorescent staining with Hoechst 33342 (blue) and PI (red). PI positive cells were quantified. Data shown are mean  $\pm$  SD from three independent experiments. \* $P$  < 0.05, \*\* $P$  < 0.01, \*\*\* $P$  < 0.001.

## MiR-135a-5p directly targets TXNIP

Bioinformatics analyses revealed that miR-135a-5p could directly interact with TXNIP 3'UTR (Figure 5A), with lower free energy score (Figure 5B). Moreover, transfection of 293T cells with miR-135a-5p mimic obviously diminished the luciferase activity of TXNIP-WT (Figure 5C). Subsequently, we overexpressed or silenced miR-135a-5p in human NP cells (Figure 5D). Overexpression of miR-135a-5p markedly diminished TXNIP levels, and an opposite effect appeared after silencing of this miRNA (Figure 5E). Collectively, the above results reveal that miR-135a-5p can directly target TXNIP.

## APN down-regulates TXNIP expression and inhibits human NP cell pyroptosis through miR-135a-5p

For validating whether APN-regulated human NP cell pyroptosis is mediated by miR-135a-5p, we first detected its expression using qRT-PCR. Contrary to TXNIP, decreased miR-135a-5p amount was seen in human degenerated NP tissue samples (Figure 6A). LPS also reduced miR-135a-5p levels within human NP cells, while its reduction was suppressed after APN overexpression (Figure 6B). Next, human NP cells were subjected to miR-135a-5p inhibitor and/or APN-expressing lentiviral vector treatment in the presence of

LPS. APN overexpression decreased TXNIP expression, which was abolished after miR-135a-5p inhibition (Figure 6C). APN-mediated down-regulation of pyroptosis-related protein expression was abrogated by miR-135a-5p knockdown (Figure 6D). Also, APN overexpression reduced extracellular IL-1 $\beta$ , IL-18 and LDH contents and pyroptotic cell death, which was reversed upon miR-135a-5p prevention (Figure 6E–6G). Taken together, APN down-regulates TXNIP expression and restrains LPS-induced human NP cell pyroptosis by enhancing miR-135a-5p levels.

## DISCUSSION

APN is produced predominantly by adipose tissue. Notably, skeletal muscle and cardiomyocytes can synthesize APN as well [22, 23]. NP is a major structure component within the IVD tissue and has the ability to generate APN. A recent study demonstrated that human degenerated IVD tissue exhibit a significant reduction in APN expression, and that treatment with APN decreases TNF- $\alpha$  production in degenerated NP cells [8]. Similar to this report, we observed decreased APN expression in degenerated NP tissue. Exposure of human NP cells to LPS could also inhibit APN expression. These findings suggest that decreased APN levels might have a causative role in IDD.

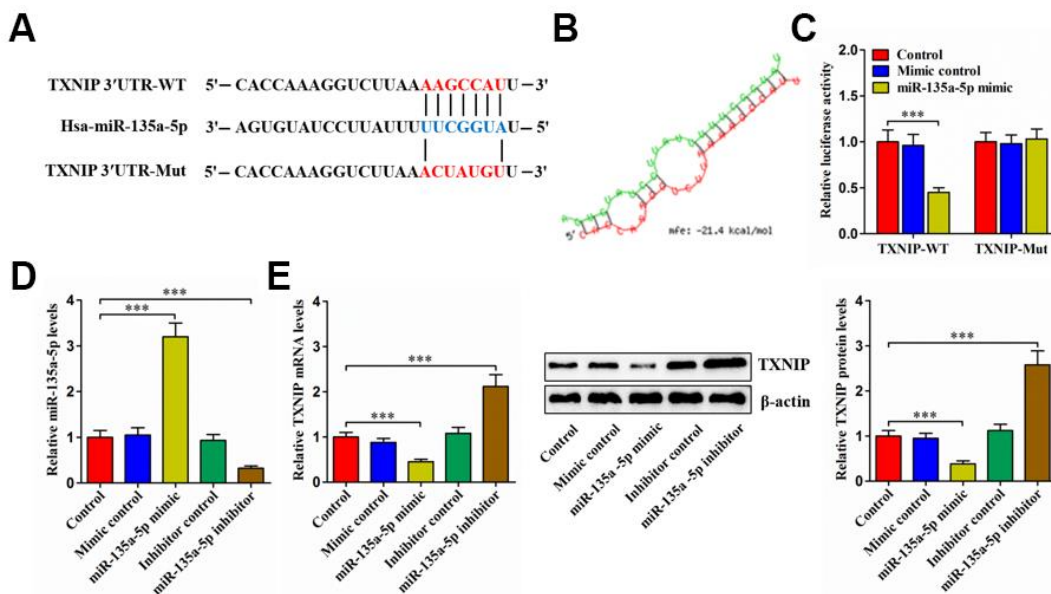


**Figure 5. TXNIP is a direct target of miR-135a-5p.** (A) Schematic of miR-135a-5p binding site in the 3'UTR of TXNIP mRNA and corresponding mutation. (B) Free energy score predicted by the RNAhybrid database. (C) The luciferase reporter plasmids (TXNIP-WT and TXNIP-Mut) were co-transfected into 293T cells with miR-135a-5p mimic or mimic control for 24 h, followed by measurement of luciferase activity. (D, E) Human NP cells were transfected with miR-135a-5p mimic/inhibitor or their negative controls for 24 h. (D) The qRT-PCR analysis of miR-135a-5p expression. (E) Detection of TXNIP expression using qRT-PCR and western blot. Data represent the mean  $\pm$  SD from three independent experiments. \*\*\* $P < 0.001$ .

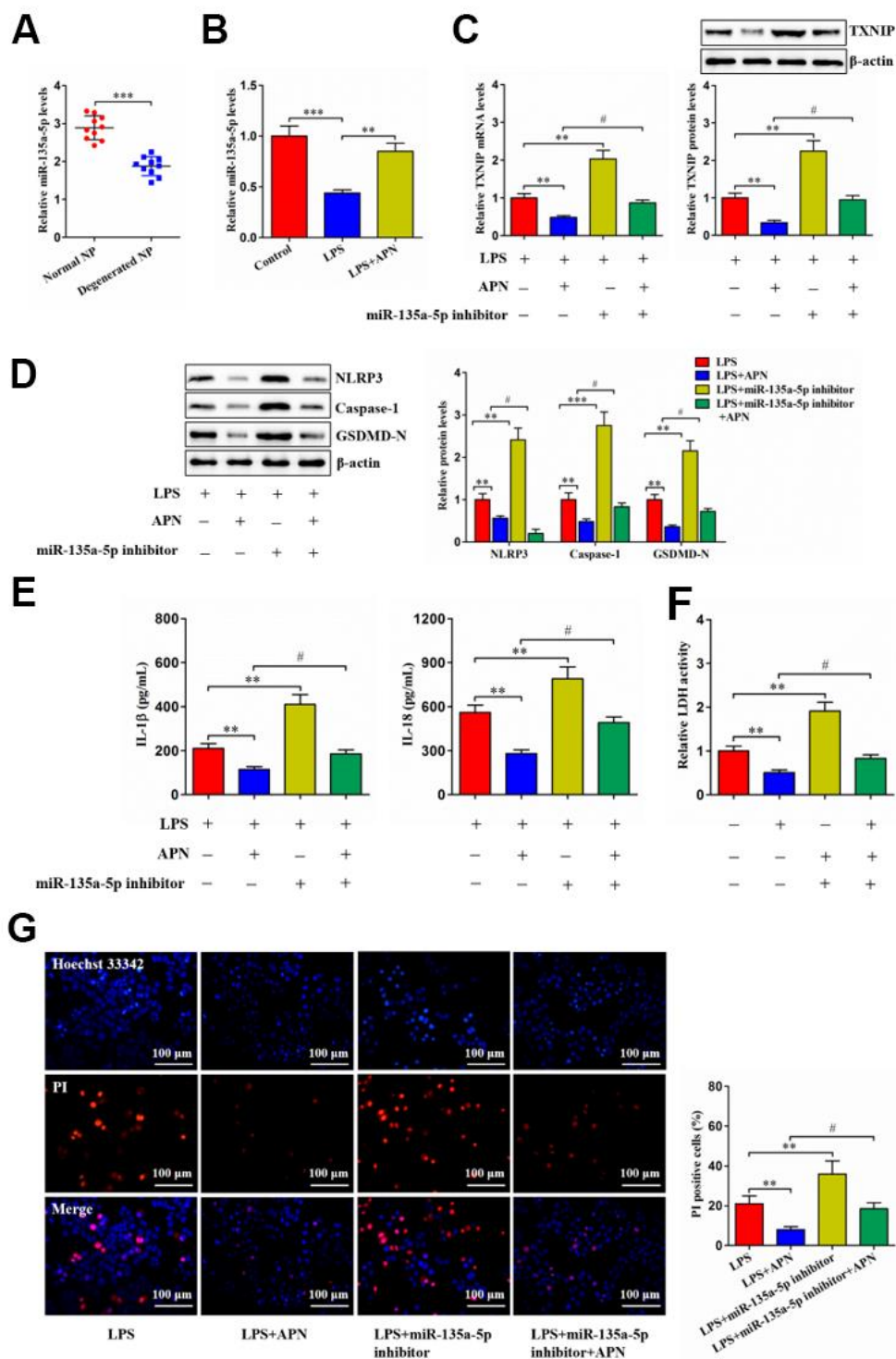


**Figure 6. APN suppresses human NP cell pyroptosis by up-regulating miR-135a-5p expression.** (A) Detection of miR-135a-5p expression in normal and degenerated human NP tissue samples using qRT-PCR ( $n=10$ ). (B) Human NP cells were treated with PBS or LPS for 12 h and then transfected with or without lentiviral vector overexpressing APN for an additional 24 h. The expression of miR-135a-5p was analyzed by qRT-PCR ( $n=3$ ). (C–G) LPS-stimulated human NP cells were transfected with or without miR-135a-5p inhibitor for 24 h, followed by transduction with APN-expressing lentivirus for another 24 h ( $n=3$ ). (C) TXNIP expression was measured using qRT-PCR and western blot. (D) Western blot was applied to determine the protein levels of NLRP3, caspase-1 and GSDMD-N. (E) Detection of IL-1 $\beta$  and IL-18 levels in the cell culture supernatants using ELISA. (F) The LDH assay kit was utilized to detect LDH activity in the cell culture supernatants. (G) Representative images of fluorescent staining with Hoechst 33342 (blue) and PI (red) and quantitative analysis of PI positive cells. The results are shown as the mean  $\pm$  SD. \*\* $P < 0.01$ , \*\*\* $P < 0.001$ , # $P < 0.05$ .



Cell pyroptosis is characterized by membrane pore formation and pro-inflammatory mediator release [24]. NP cell pyroptosis not only triggers inflammatory response within the IVD, but also promotes extracellular matrix degradation [25]. Prevention of NP cell pyroptosis ameliorates IDD in animal models [18]. APN was shown to suppress pyroptosis in aortic epithelial cells [10], vascular smooth muscle cells [11], and hepatocytes [26]. Similarly, we found that lentiviral vector expressing APN diminished pyroptosis-related protein, IL-1 $\beta$ , IL-18 and LDH levels as well as inhibited death occurrence in human NP cells challenged with LPS. Thus, APN plays a protective role in NP cell pyroptosis.

TXNIP is a negative regulator of thioredoxin. In addition to involving oxidative stress, TXNIP serves as a binding partner to NLRP3 [27, 28]. Recently, Yu et al. reported that TXNIP is up-regulated in human degenerated NP tissue samples [29]. Overexpression of TXNIP promotes NP cell pyroptosis and accelerate mouse IVD degeneration by binding to NLRP3; however, an opposite effect is observed when TXNIP is knocked down [18]. In this study, incremental TXNIP expression was seen in human degenerated NP tissue. LPS stimulation also up-regulated TXNIP expression in human NP cells. Importantly, overexpression of APN decreased TXNIP levels and inhibited its interaction with NLRP3 in human NP cells challenged with LPS. APN-induced reduction of NP cell pyroptosis was also alleviated by TXNIP overexpression. Therefore, suppression of NP cell pyroptosis by APN requires TXNIP.

MiRNAs exert biological functions via silencing their target genes [30]. Dysregulated miRNAs take part in inflammatory diseases and IDD [31, 32]. In PC12 cells treated with oxygen-glucose deprivation/reoxygenation, lncRNA SOX2 overlapping transcript promotes the production of pro-inflammatory mediators by sponging miR-135a-5p [33]. Additionally, transfection of HASMCs with miR-135a-5p mimic was shown to attenuate inflammatory cytokine levels [15]. Our present study revealed that miR-135a-5p targeted TXNIP. Importantly, APN-induced inhibition of TXNIP expression and NP cell pyroptosis was attenuated after miR-135a-5p inhibitor transfection. Thus, our data imply that APN-regulated TXNIP expression and NP cell pyroptosis is mediated, at least in part, by miR-135a-5p.

Although this study has clearly demonstrated that APN is protective against LPS-induced human NP cell pyroptosis, there are several limitations in our research. Oxidative stress is known to promote IDD progression besides inflammation [34, 35]. TXNIP also plays a vital role in mediating oxidative stress [36]. Whether APN can affect oxidative stress in NP cells needs to be determined in future research. There is a lack of more immunostaining test for pyroptosis markers, such as caspase-1, to further confirm the occurrence of cell pyroptosis in NP tissue samples and cultured cells. In addition, we do not observe the impact of APN on IDD in animal models.

In conclusion, APN exerts an inhibitory effect on NP cell pyroptosis, which is dependent on the miR-135a-5p/TXNIP signaling pathway (Figure 7). These findings

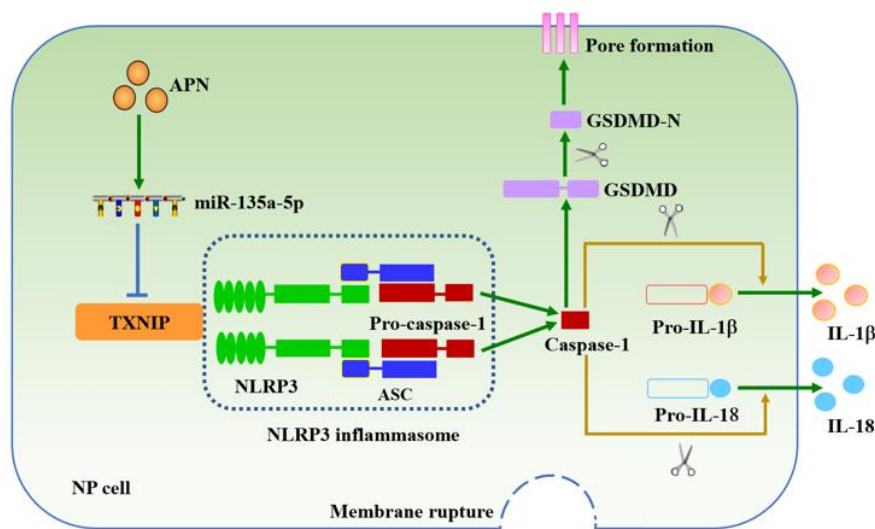


**Figure 7. Schematic diagram of APN-induced prevention of human NP cell pyroptosis.** APN increases miR-135a-5p levels and then down-regulates TXNIP expression, leading to decreased interaction between TXNIP and NLRP3 in human NP cells stimulated with LPS. Inactivation of the NLRP3 inflammasome inhibits membrane pore formation and subsequent release of IL-1 $\beta$  and IL-18.

deepen our understanding for the role of APN in the pathogenesis of IDD. Targeting APN could be a potential strategy to prevent and treat IDD.

## Abbreviations

IDD: intervertebral disc degeneration; IL: interleukin; NP: nucleus pulposus; APN: adiponectin; NLRP3: nucleotide-binding oligomerization domain-like receptor protein 3; LPS: lipopolysaccharide; miRNAs: microRNAs; TXNIP: thioredoxin-interacting protein; PI: propidium iodide; GSDMD-N: Gasdermin N-terminal fragment; LDH: lactate dehydrogenase.

## AUTHOR CONTRIBUTIONS

Jian Zhang conceived the idea and designed the experimental protocols. Shuang Wu, Shida Liu, Rui Huang, Youbing Zhou, and Yongcheng Zou performed the experiments, collected the data and conducted statistical analysis. Shuang Wu wrote the manuscript. Wei Yang and Jian Zhang revised the manuscript. All authors read and approved the final manuscript.

## CONFLICTS OF INTEREST

The authors declare that they have no conflicts of interest.

## ETHICAL STATEMENT AND CONSENT

The collection of NP tissue samples was approved by the Ethics Committee of the First Affiliated Hospital of University of South China, and informed consent was obtained from each subject.

## FUNDING

This study was supported by research funds from the Natural Science Foundation in Hunan Province (2021JJ50099), the Scientific Research Project of Hunan Provincial Department of Education (22C0206), Health Commission of Hunan Province (D202304079664) and Clinical Medical Technology Innovation Guidance Project of Hunan Province (2020SK51819) in China.

## REFERENCES

1. Zhang F, Zhao X, Shen H, Zhang C. Molecular mechanisms of cell death in intervertebral disc degeneration (Review). *Int J Mol Med*. 2016; 37:1439–48. <https://doi.org/10.3892/ijmm.2016.2573> PMID:27121482
2. Lyu FJ, Cui H, Pan H, Mc Cheung K, Cao X, Iatridis JC, Zheng Z. Painful intervertebral disc degeneration and inflammation: from laboratory evidence to clinical interventions. *Bone Res*. 2021; 9:7. <https://doi.org/10.1038/s41413-020-00125-x> PMID:33514693
3. Zhang QX, Guo D, Wang FC, Ding WY. Necrosulfonamide (NSA) protects intervertebral disc degeneration via necroptosis and apoptosis inhibition. *Eur Rev Med Pharmacol Sci*. 2020; 24:2683–91. [https://doi.org/10.26355/eurev\\_202003\\_20538](https://doi.org/10.26355/eurev_202003_20538) PMID:32196619
4. Zhou Y, Deng M, Su J, Zhang W, Liu D, Wang Z. The Role of miR-31-5p in the Development of Intervertebral Disc Degeneration and Its Therapeutic Potential. *Front Cell Dev Biol*. 2021; 9:633974. <https://doi.org/10.3389/fcell.2021.633974> PMID:33816484
5. Zhao K, An R, Xiang Q, Li G, Wang K, Song Y, Liao Z, Li S, Hua W, Feng X, Wu X, Zhang Y, Das A, Yang C. Acid-sensing ion channels regulate nucleus pulposus cell inflammation and pyroptosis via the NLRP3 inflammasome in intervertebral disc degeneration. *Cell Prolif*. 2021; 54:e12941. <https://doi.org/10.1111/cpr.12941> PMID:33111436
6. Zhang J, Zhang J, Zhang Y, Liu W, Ni W, Huang X, Yuan J, Zhao B, Xiao H, Xue F. Mesenchymal stem cell-derived exosomes ameliorate intervertebral disc degeneration through inhibiting pyroptosis. *J Cell Mol Med*. 2020; 24:11742–54. <https://doi.org/10.1111/jcmm.15784> PMID:32860495
7. Choi HM, Doss HM, Kim KS. Multifaceted Physiological Roles of Adiponectin in Inflammation and Diseases. *Int J Mol Sci*. 2020; 21:1219. <https://doi.org/10.3390/ijms21041219> PMID:32059381
8. Yuan B, Huang L, Yan M, Zhang S, Zhang Y, Jin B, Ma Y, Luo Z. Adiponectin Downregulates TNF- $\alpha$  Expression in Degenerated Intervertebral Discs. *Spine (Phila Pa 1976)*. 2018; 43:E381–9. <https://doi.org/10.1097/BRS.0000000000002364> PMID:28767622
9. Khabour OF, Abu-Rumeh L, Al-Jarrah M, Jamous M, Alhashimi F. Association of adiponectin protein and ADIPOQ gene variants with lumbar disc degeneration. *Exp Ther Med*. 2014; 8:1340–4. <https://doi.org/10.3892/etm.2014.1909> PMID:25187851
10. Zhang L, Yuan M, Zhang L, Wu B, Sun X. Adiponectin alleviates NLRP3-inflammasome-mediated pyroptosis of aortic endothelial cells by inhibiting FoxO4 in arteriosclerosis. *Biochem Biophys Res Commun*. 2019; 514:266–72.

- <https://doi.org/10.1016/j.bbrc.2019.04.143>  
PMID:[31030940](https://pubmed.ncbi.nlm.nih.gov/31030940/)
11. Duan H, Zhang X, Song R, Liu T, Zhang Y, Yu A. Upregulation of miR-133a by adiponectin inhibits pyroptosis pathway and rescues acute aortic dissection. *Acta Biochim Biophys Sin (Shanghai)*. 2020; 52:988–97.  
<https://doi.org/10.1093/abbs/gmaa078>  
PMID:[32634201](https://pubmed.ncbi.nlm.nih.gov/32634201/)
  12. Wang C, Wang WJ, Yan YG, Xiang YX, Zhang J, Tang ZH, Jiang ZS. MicroRNAs: New players in intervertebral disc degeneration. *Clin Chim Acta*. 2015; 450:333–41.  
<https://doi.org/10.1016/j.cca.2015.09.011>  
PMID:[26368266](https://pubmed.ncbi.nlm.nih.gov/26368266/)
  13. Wang WJ, Yang W, Ouyang ZH, Xue JB, Li XL, Zhang J, He WS, Chen WK, Yan YG, Wang C. MiR-21 promotes ECM degradation through inhibiting autophagy via the PTEN/akt/mTOR signaling pathway in human degenerated NP cells. *Biomed Pharmacother*. 2018; 99:725–34.  
<https://doi.org/10.1016/j.biopha.2018.01.154>  
PMID:[29710470](https://pubmed.ncbi.nlm.nih.gov/29710470/)
  14. Wang J, Liu X, Sun B, Du W, Zheng Y, Sun Y. Upregulated miR-154 promotes ECM degradation in intervertebral disc degeneration. *J Cell Biochem*. 2019; 120:11900–7.  
<https://doi.org/10.1002/jcb.28471> PMID:[30825225](https://pubmed.ncbi.nlm.nih.gov/30825225/)
  15. Li C, Zhang S, Chen X, Ji J, Yang W, Gui T, Gai Z, Li Y. Farnesoid X receptor activation inhibits TGFBR1/TAK1-mediated vascular inflammation and calcification via miR-135a-5p. *Commun Biol*. 2020; 3:327.  
<https://doi.org/10.1038/s42003-020-1058-2>  
PMID:[32581266](https://pubmed.ncbi.nlm.nih.gov/32581266/)
  16. Zhou R, Tardivel A, Thorens B, Choi I, Tschopp J. Thioredoxin-interacting protein links oxidative stress to inflammasome activation. *Nat Immunol*. 2010; 11:136–40.  
<https://doi.org/10.1038/ni.1831> PMID:[20023662](https://pubmed.ncbi.nlm.nih.gov/20023662/)
  17. Ke R, Wang Y, Hong S, Xiao L. Endoplasmic reticulum stress related factor IRE1 $\alpha$  regulates TXNIP/NLRP3-mediated pyroptosis in diabetic nephropathy. *Exp Cell Res*. 2020; 396:112293.  
<https://doi.org/10.1016/j.yexcr.2020.112293>  
PMID:[32950473](https://pubmed.ncbi.nlm.nih.gov/32950473/)
  18. Zhou Y, Chen Z, Yang X, Cao X, Liang Z, Ma H, Zhao J. Morin attenuates pyroptosis of nucleus pulposus cells and ameliorates intervertebral disc degeneration via inhibition of the TXNIP/NLRP3/Caspase-1/IL-1 $\beta$  signaling pathway. *Biochem Biophys Res Commun*. 2021; 559:106–12.  
<https://doi.org/10.1016/j.bbrc.2021.04.090>  
PMID:[33933989](https://pubmed.ncbi.nlm.nih.gov/33933989/)
  19. He D, Zhou M, Bai Z, Wen Y, Shen J, Hu Z. Propionibacterium acnes induces intervertebral disc degeneration by promoting nucleus pulposus cell pyroptosis via NLRP3-dependent pathway. *Biochem Biophys Res Commun*. 2020; 526:772–9.  
<https://doi.org/10.1016/j.bbrc.2020.03.161>  
PMID:[32265028](https://pubmed.ncbi.nlm.nih.gov/32265028/)
  20. Wang G, Chen JJ, Deng WY, Ren K, Yin SH, Yu XH. CTRP12 ameliorates atherosclerosis by promoting cholesterol efflux and inhibiting inflammatory response via the miR-155-5p/LXR $\alpha$  pathway. *Cell Death Dis*. 2021; 12:254.  
<https://doi.org/10.1038/s41419-021-03544-8>  
PMID:[33692340](https://pubmed.ncbi.nlm.nih.gov/33692340/)
  21. Jiang Y, Liu H, Yu H, Zhou Y, Zhang J, Xin W, Li Y, He S, Ma C, Zheng X, Zhang L, Zhao X, Wu B, et al. Circular RNA Calm4 Regulates Hypoxia-Induced Pulmonary Arterial Smooth Muscle Cells Pyroptosis via the Circ-Calm4/miR-124-3p/PDCD6 Axis. *Arterioscler Thromb Vasc Biol*. 2021; 41:1675–93.  
<https://doi.org/10.1161/ATVBAHA.120.315525>  
PMID:[33657879](https://pubmed.ncbi.nlm.nih.gov/33657879/)
  22. Delaigle AM, Jonas JC, Bauche IB, Cornu O, Brichard SM. Induction of adiponectin in skeletal muscle by inflammatory cytokines: *in vivo* and *in vitro* studies. *Endocrinology*. 2004; 145:5589–97.  
<https://doi.org/10.1210/en.2004-0503> PMID:[15319349](https://pubmed.ncbi.nlm.nih.gov/15319349/)
  23. Piñeiro R, Iglesias MJ, Gallego R, Raghay K, Eiras S, Rubio J, Diéguez C, Gualillo O, González-Juanatey JR, Lago F. Adiponectin is synthesized and secreted by human and murine cardiomyocytes. *FEBS Lett*. 2005; 579:5163–9.  
<https://doi.org/10.1016/j.febslet.2005.07.098>  
PMID:[16140297](https://pubmed.ncbi.nlm.nih.gov/16140297/)
  24. Bergsbaken T, Fink SL, den Hartigh AB, Loomis WP, Cookson BT. Coordinated host responses during pyroptosis: caspase-1-dependent lysosome exocytosis and inflammatory cytokine maturation. *J Immunol*. 2011; 187:2748–54.  
<https://doi.org/10.4049/jimmunol.1100477>  
PMID:[21804020](https://pubmed.ncbi.nlm.nih.gov/21804020/)
  25. Chao-Yang G, Peng C, Hai-Hong Z. Roles of NLRP3 inflammasome in intervertebral disc degeneration. *Osteoarthritis Cartilage*. 2021; 29:793–801.  
<https://doi.org/10.1016/j.joca.2021.02.204>  
PMID:[33609693](https://pubmed.ncbi.nlm.nih.gov/33609693/)
  26. Khakurel A, Park PH. Globular adiponectin protects hepatocytes from tunicamycin-induced cell death via modulation of the inflammasome and heme oxygenase-1 induction. *Pharmacol Res*. 2018; 128:231–43.  
<https://doi.org/10.1016/j.phrs.2017.10.010>  
PMID:[29079428](https://pubmed.ncbi.nlm.nih.gov/29079428/)

27. Jiang J, Shi Y, Cao J, Lu Y, Sun G, Yang J. Role of ASM/Cer/TXNIP signaling module in the NLRP3 inflammasome activation. *Lipids Health Dis.* 2021; 20:19.  
<https://doi.org/10.1186/s12944-021-01446-4>  
PMID:[33612104](https://pubmed.ncbi.nlm.nih.gov/33612104/)
28. Wang L, Zhao H, Xu H, Liu X, Chen X, Peng Q, Xiao M. Targeting the TXNIP-NLRP3 interaction with PSSM1443 to suppress inflammation in sepsis-induced myocardial dysfunction. *J Cell Physiol.* 2021; 236:4625–39.  
<https://doi.org/10.1002/jcp.30186>  
PMID:[33452697](https://pubmed.ncbi.nlm.nih.gov/33452697/)
29. Yu L, Hao Y, Xu C, Zhu G, Cai Y. LINC00969 promotes the degeneration of intervertebral disk by sponging miR-335-3p and regulating NLRP3 inflammasome activation. *IUBMB Life.* 2019; 71:611–8.  
<https://doi.org/10.1002/iub.1989>  
PMID:[30592131](https://pubmed.ncbi.nlm.nih.gov/30592131/)
30. Vishnoi A, Rani S. MiRNA Biogenesis and Regulation of Diseases: An Overview. *Methods Mol Biol.* 2017; 1509:1–10.  
[https://doi.org/10.1007/978-1-4939-6524-3\\_1](https://doi.org/10.1007/978-1-4939-6524-3_1)  
PMID:[27826912](https://pubmed.ncbi.nlm.nih.gov/27826912/)
31. Cazzanelli P, Wuertz-Kozak K. MicroRNAs in Intervertebral Disc Degeneration, Apoptosis, Inflammation, and Mechanobiology. *Int J Mol Sci.* 2020; 21:3601.  
<https://doi.org/10.3390/ijms21103601>  
PMID:[32443722](https://pubmed.ncbi.nlm.nih.gov/32443722/)
32. Guo HY, Guo MK, Wan ZY, Song F, Wang HQ. Emerging evidence on noncoding-RNA regulatory machinery in intervertebral disc degeneration: a narrative review. *Arthritis Res Ther.* 2020; 22:270.  
<https://doi.org/10.1186/s13075-020-02353-2>  
PMID:[33198793](https://pubmed.ncbi.nlm.nih.gov/33198793/)
33. Wang C, Hu F. Long noncoding RNA SOX2OT silencing alleviates cerebral ischemia-reperfusion injury via miR-135a-5p-mediated NR3C2 inhibition. *Brain Res Bull.* 2021; 173:193–202.  
<https://doi.org/10.1016/j.brainresbull.2021.05.018>  
PMID:[34022287](https://pubmed.ncbi.nlm.nih.gov/34022287/)
34. Feng C, Yang M, Lan M, Liu C, Zhang Y, Huang B, Liu H, Zhou Y. ROS: Crucial Intermediators in the Pathogenesis of Intervertebral Disc Degeneration. *Oxid Med Cell Longev.* 2017; 2017:5601593.  
<https://doi.org/10.1155/2017/5601593> PMID:[28392887](https://pubmed.ncbi.nlm.nih.gov/28392887/)
35. Zhang GZ, Deng YJ, Xie QQ, Ren EH, Ma ZJ, He XG, Gao YC, Kang XW. Sirtuins and intervertebral disc degeneration: Roles in inflammation, oxidative stress, and mitochondrial function. *Clin Chim Acta.* 2020; 508:33–42.  
<https://doi.org/10.1016/j.cca.2020.04.016>  
PMID:[32348785](https://pubmed.ncbi.nlm.nih.gov/32348785/)
36. Zhou J, Chng WJ. Roles of thioredoxin binding protein (TXNIP) in oxidative stress, apoptosis and cancer. *Mitochondrion.* 2013; 13:163–9.  
<https://doi.org/10.1016/j.mito.2012.06.004>  
PMID:[22750447](https://pubmed.ncbi.nlm.nih.gov/22750447/)

## SUPPLEMENTARY MATERIALS

### Supplementary Table

**Supplementary Table 1. Summary of clinical and demographic features of patients.**

| <b>Subject number</b> | <b>Gender</b> | <b>Age (years)</b> | <b>Level</b> | <b>Pfirmann grading</b> |
|-----------------------|---------------|--------------------|--------------|-------------------------|
| Normal control group  |               |                    |              |                         |
| 1                     | Male          | 18                 | L1/2         | II                      |
| 2                     | Male          | 16                 | L4/5         | II                      |
| 3                     | Female        | 20                 | L2/3         | II                      |
| 4                     | Male          | 21                 | L2/3         | II                      |
| 5                     | Male          | 19                 | L4/5         | II                      |
| 6                     | Male          | 24                 | L3/4         | II                      |
| 7                     | Female        | 22                 | L3/4         | II                      |
| 8                     | Male          | 23                 | L4/5         | II                      |
| 9                     | Female        | 25                 | L2/3         | II                      |
| 10                    | Female        | 18                 | L4/5         | II                      |
| IDD group             |               |                    |              |                         |
| 1                     | Male          | 57                 | L4/5         | IV                      |
| 2                     | Male          | 40                 | L5/S1        | V                       |
| 3                     | Female        | 45                 | L4/5         | V                       |
| 4                     | Female        | 60                 | L4/5         | IV                      |
| 5                     | Male          | 55                 | L3/4         | IV                      |
| 6                     | Female        | 54                 | L4/5         | IV                      |
| 7                     | Female        | 57                 | L5/S1        | V                       |
| 8                     | Male          | 48                 | L5/S1        | IV                      |
| 9                     | Female        | 58                 | L3/4         | IV                      |
| 10                    | Male          | 51                 | L4/5         | V                       |